

Electromagnetically Induced Transparency in ^6Li

J Fuchs, G J Duffy, W J Rowlands and A M Akulshin

ARC Centre of Excellence for Quantum Atom Optics, Centre for Atom Optics and Ultrafast Spectroscopy, Swinburne University of Technology, Melbourne, Victoria 3122, Australia

E-mail: jfuchs@swin.edu.au

Abstract. We report electromagnetically induced transparency for the D1 and D2 lines in ^6Li in both a vapour cell and an atomic beam. Electromagnetically induced transparency is created using co-propagating mutually coherent laser beams with a frequency difference equal to the hyperfine ground state splitting of 228.2 MHz. The effects of various optical polarization configurations and applied magnetic fields are investigated. In addition, we apply an optical Ramsey spectroscopy technique which further reduces the observed resonance width.

PACS numbers: 32.10.Fn, 32.30.Jc, 32.80.Qk

Submitted to: *J. Phys. B: At. Mol. Phys.*

1. Introduction

Electromagnetically Induced Transparency (EIT) is of great interest due to its wide application in lasing without inversion (Zibrov *et al* 1995), control of light propagation (slow light) (Matsko *et al* 2001) and enhanced Kerr nonlinearity (Harris and Hau 1999, Akulshin *et al* 2003). The concept of a non-absorbing dark state is the key basis of light storage (Lukin 2003). Lithium has two stable isotopes, ${}^6\text{Li}$ and ${}^7\text{Li}$ (7.5 % and 92.5 % natural abundance, respectively). Magnus *et al* (Magnus *et al* 2005) reported the first study of EIT on the D1 and D2 lines of ${}^7\text{Li}$ in a vapour. In this paper we present EIT in ${}^6\text{Li}$ performed on both the D1 and D2 lines using several nonlinear techniques, paying particular attention to a comparison between the EIT resonances obtained on the D1 and D2 lines.

EIT is a phenomenon in which an opaque atomic medium is turned into a transparent one in the presence of a control laser field (Harris 1997). When two Zeeman sub-levels or two hyperfine levels in an atomic ground state are coupled by light to a common excited state, the interference between amplitudes of alternative transition paths can substantially reduce the absorption. The atoms are pumped by the laser light into a coherent superposition of the ground state sublevels which constitutes a non-absorbing state decoupled from the laser field. This phenomenon is also known as coherent population trapping, e.g., (Arimondo 1996). The absorption of the probe exhibits a narrow dip that has a sub-natural linewidth ultimately determined by the relaxation time of the ground state sublevels. The refractive index of the coherent atomic medium reveals extremely steep normal dispersion in the vicinity of the EIT resonance, so that the group velocity of light in such an atomic medium can be dramatically reduced (Schmidt *et al* 1996).

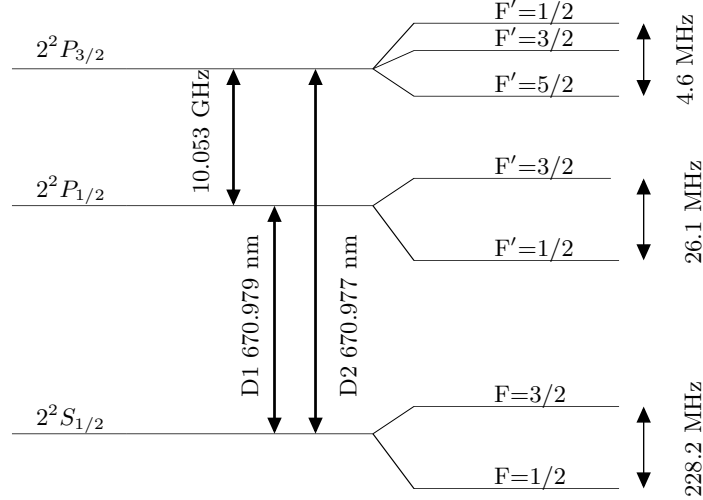


Figure 1. A schematic energy level diagram for ${}^6\text{Li}$.

EIT in alkali atoms with half-integer total angular momentum ($F=J+I$, $J=L\pm 1/2$) have not, to our knowledge, been previously investigated. A schematic diagram of the relevant atomic energy levels is shown in figure 1. The level structure of ${}^6\text{Li}$ is somewhat different to other alkali atoms that have been used to study EIT

and other effects related to ground state coherence. There are only three sublevels in the $2^2P_{3/2}$ state in comparison with four sublevels for all other alkali $n^2P_{3/2}$ states.

The strongest optical transitions of ${}^6\text{Li}$ are two electric dipole transitions $2^2S_{1/2} \rightarrow 2^2P_{1/2}$ (D1 line) and $2^2S_{1/2} \rightarrow 2^2P_{3/2}$ (D2 line) which are separated by a fine structure splitting of ~ 10 GHz. Of all the alkali atoms ${}^6\text{Li}$ has the smallest hyperfine splitting in both the ground and excited states. The hyperfine splitting of the $2^2S_{1/2}$ ground state, 228.2 MHz (Walls *et al* 2003), is much less than the Doppler width of the D lines near room temperature. But, more interestingly, the hyperfine splitting of the $2^2P_{3/2}$ state is smaller than the 5.9 MHz (McAlexander *et al* 1996) natural width of the optical transition. Thus, every atom has comparable probabilities, independent of the atomic velocity, of being excited via different transitions on the D2 line. This unique situation for alkali atoms allows analyzing a role of additional optical transitions, which do not contribute to the preparation of a non-absorbing coherent state responsible for EIT. This study could be useful for optimization of EIT resonances widely used for metrological applications (Knappe *et al* 2005).

The ultimate width of an EIT resonance also depends on the mutual coherence of the probe and control laser fields (Arimondo 1996). In the case of Cs and Rb, which have large ground state splitting, several methods can be used to produce two phase-stable laser fields such as high frequency acousto-optical modulators (AOM), two phase-locked lasers, applying current modulation to laser diodes and the use of electro-optic modulators (Wynands *et al* 1999). High frequency AOMs are expensive while phase locking at precise frequency offset and current modulation at high frequencies are experimentally not simple. However, in the case of lithium the ground state splitting is relatively small and mutually coherent probe and control fields can be easily prepared from the same laser using a low-cost AOM in a double pass configuration, thus eliminating laser linewidth contribution.

2. Experimental Set-up

An external cavity diode laser (ECDL) (Toptica DL 100) is used as the source of the resonant optical field which has an output power of 15 mW and a linewidth of approximately 1 MHz. Using the so-called feed-forward technique, where both the diode current and the grating position are varied, a fine frequency tuning range of over 20 GHz is obtained. The vapour cell consists of a stainless steel crossed tube configuration with a flexible bellow construction and viewports on each end of the 30 cm horizontal arm. Using a thermocoax element the centre part of the vapour cell is heated to 350 °C yielding a maximum unsaturated absorption of about 20%. At this temperature the Doppler width is 3.5 GHz. Lithium vapour is limited by its mean free path to the centre part of the tube, protecting the viewports from becoming coated with lithium. To further reduce this problem we heat the viewports to 120 °C.

Saturation spectroscopy of lithium vapour provides an excellent frequency reference for our experiments in an atomic beam. Figure 2 shows typical Doppler-free spectra of ${}^6\text{Li}$ with a frequency scan over both the D1 (figure 2 (a)) and D2 (figure 2 (b)) lines. The inset shows a close up of the D2 line whose outer peaks correspond to the $F = 3/2 \rightarrow F' = 5/2, 3/2, 1/2$ and $F = 1/2 \rightarrow F' = 3/2, 1/2$ transitions, respectively. The reduction in absorption of the probe at these outer peaks is due to the saturation of the transition by the pump beam. The enhancement in absorption of the crossover dip is due to compensation of optical hyperfine pumping, which occurs when the pump and probe laser are resonant with both ground state

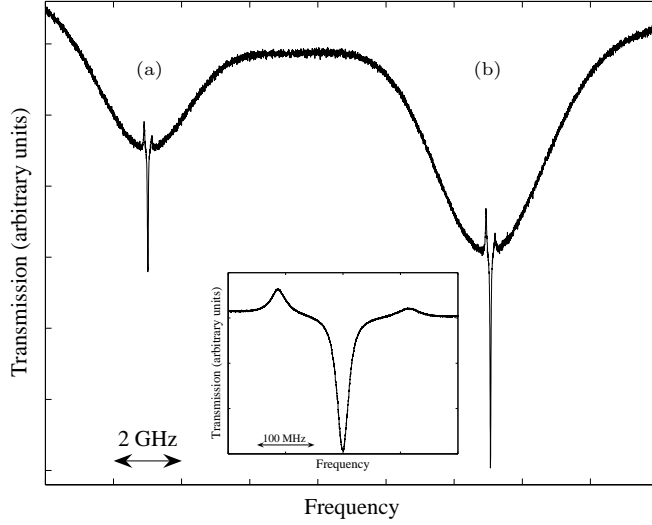


Figure 2. Doppler-free spectrum of the D1 (a) and D2 (b) lines in ${}^6\text{Li}$. The inset shows a close-up of the scan across the D2 line. The outer two peaks in the inset correspond to $F = 3/2 \rightarrow F' = 5/2, 3/2, 1/2$ and $F = 1/2 \rightarrow F' = 3/2, 1/2$ transitions.

sublevels at the same time. When applying higher intensities the spectroscopy of the D1 line resembles the spectroscopy of the D2 line (inset in figure 2). The width of the crossover peak in the D2 line is ≈ 25 MHz. The contrast ratio of the crossover peak with respect to the Doppler broadened resonance is $\approx 100\%$.

Figure 3 shows the experimental set-up used for EIT experiments in both the vapour cell and atomic beam. The EIT resonances are usually observed with a bichromatic laser beam consisting of two components with tunable frequency offset changing in the vicinity of the ground state hyperfine splitting. The ECDL (master laser) is used to injection lock a diode laser (slave 1) which injection locks two additional diode lasers (slave 2 and slave 3). The master laser is tuned to either the D1 or D2 line. For the vapour cell experiments the master laser is not actively stabilized since its long-term drift is small compared to the Doppler width. However for the atomic beam experiments the master laser is actively locked to the crossover of the saturated absorption lines. Radiation of slave 3 is used as a pump beam for coupling states between the ground state $F = 1/2$ and the excited levels in the D1 or D2 line. Laser light from slave 2 which is resonant with the $F = 3/2 \rightarrow F'$ transitions (either D1 or D2 line) is used as a probe beam. The probe laser frequency is scanned over ≈ 25 MHz while the frequency of the pump laser is fixed. They are overlapped on a non-polarizing beam splitting cube and expanded to a beam diameter of 5 mm for the vapour cell and 18 mm for the atomic beam experiments.

3. Vapour Cell EIT

By tailoring the optical frequencies present we performed experiments on EIT in both a vapour cell and an atomic beam. To obtain hyperfine ground state coherence we

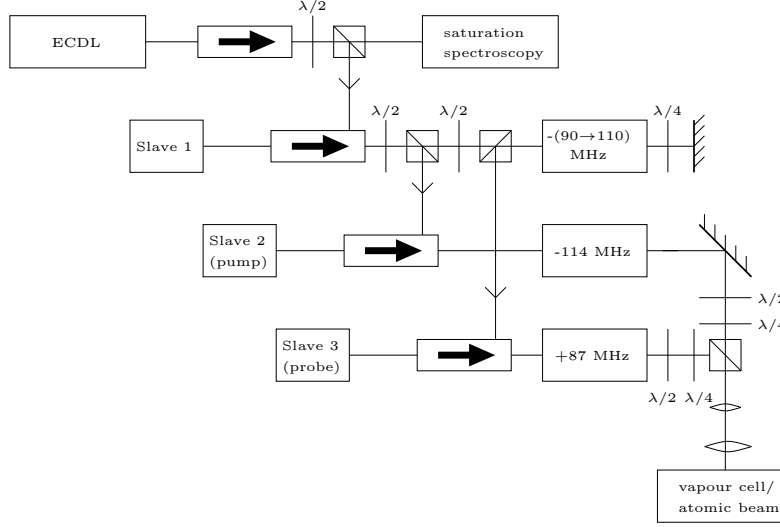


Figure 3. Experimental set-up for the EIT experiments in both the vapour cell and the atomic beam. The ECDL is tuned to either the D1 or D2 line. Three slave lasers were injection locked to the master laser. Where necessary, the frequencies were shifted using AOMs. The frequency difference sweep of the pump and probe laser was generated by the AOM in double pass. The typical frequencies used in the AOMs are shown in the above figure. Note that the saturation spectroscopy is only used in conjunction with the atomic beam experiment.

use mutually coherent laser fields whose frequencies are separated by the hyperfine splitting of the ground state. The pump and probe are sent through the vapour cell with intensities of 8 mW/cm^2 and 2 mW/cm^2 respectively. To improve the signal to noise ratio the pump is amplitude modulated by means of a mechanical chopper (1 kHz) and the probe is detected using a lock-in amplifier. For the results shown here, both beams are linearly polarized and orthogonal to each other.

3.1. Results

Figure 4 shows absorption plots of the D1 and D2 lines as a function of frequency difference between the collinear pump and probe beams. With no externally applied magnetic field a single absorption dip at a frequency difference of 228 MHz is observed (figure 4 (a) and 4 (c)). The width of these resonances is approximately 4 MHz which is less than the natural width of 5.9 MHz. The amplitudes for the D2 line are notably weaker than for the D1 line. This is due to destructive excitations via cycling transitions which do not contribute to the preparation of dark coherent states. This is in agreement with the results of Stähler *et al* (Stähler *et al* 2002) and Magnus *et al* (Magnus *et al* 2005) which show greater contrast in the dark resonance in the D1 line than the D2 line of ^{85}Rb and ^7Li , respectively.

It is difficult to compare the width of the EIT resonances obtained for both lines because any ambient magnetic field can introduce additional broadening. To investigate the possible ambient field broadening an external homogeneous magnetic field (approximately 5 G) was applied perpendicular to the laser beam $\vec{B} \perp \vec{k}$. The

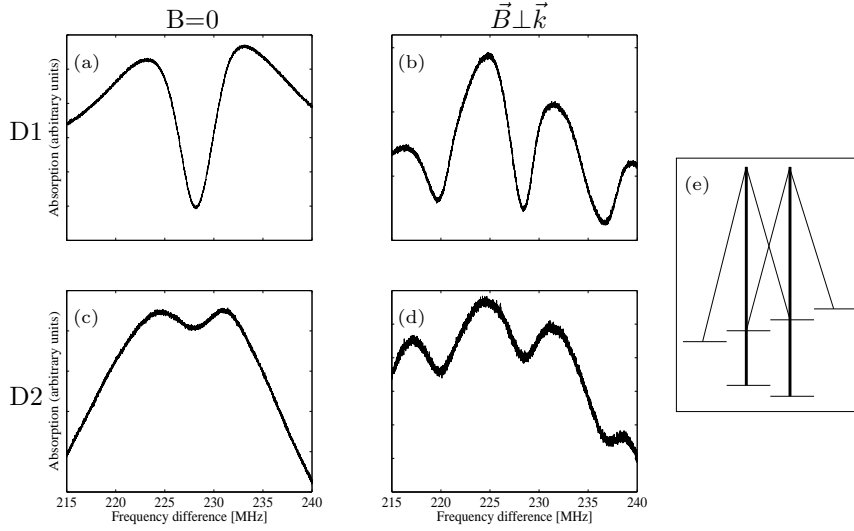


Figure 4. Absorption of the D1 (a and b) and D2 (c and d) line as a function of frequency difference between the pump and probe. (a) and (c): $B = 0$, (b) and (d) have a magnetic field of ≈ 5 G perpendicular to the laser light. (e) shows the Raman transitions responsible for coupling the ground state Zeeman sublevels for each of the resonances in (b and d). The thicker lines represent the pump laser which is tuned to the $F = 1/2 \rightarrow F'$ transitions.

magnetic field removes the degeneracy of the Zeeman levels, splitting the sub-natural EIT resonance (figure 4 (b and d)). The applied magnetic field also introduces a convenient quantization axis. The pump light with linear polarization parallel to the magnetic field can produce π transitions, while the probe with orthogonal linear polarization excites the σ^\pm transitions (figure 4 (e)). The $m = 0 \rightarrow m' = 0$ type Raman transition, which is magnetic field insensitive in the linear Zeeman approximation, does not exist for ^6Li , however, the Raman transitions $F = 1/2$ ($m = 1/2$) $\rightarrow F' = 3/2$ ($m' = -1/2$) and $F = 1/2$ ($m = -1/2$) $\rightarrow F' = 1/2$ ($m' = 1/2$) are also magnetic field insensitive, because the Zeeman shift of the upper and lower magnetic sub-levels are almost equal. Thus, the EIT dip in absorption, which remains unshifted at 228 MHz frequency difference with increasing magnetic field is due to the above mentioned Raman transitions. The width of this EIT resonance for the D1 line is approximately 3 MHz. Both outer dips are symmetrically shifted by 2Δ from the unshifted centre dip, where $\Delta = \mu_B g_F B / h$, μ_B is the Bohr magneton, h is Planck's constant and g_F is the Landé factor. The width of the outer dips are 25% larger than the width of the unshifted dip due to spatial inhomogeneities in the magnetic field.

We reduced the intensities of the pump and probe lasers but observed no change in the width of the EIT resonances which implies that the width is not limited by power broadening. Although Li-Li collisions are negligible, collisions with residual background gases may cause spin depolarizing collisions of the ground states which possibly contribute to the EIT width. The resolution is further limited by finite interaction (transit) time. The spectroscopy of atoms in a metal vapour cell has the limitations of randomly directed velocities (i.e. Doppler broadening), field

inhomogeneities and high collision rates.

4. Atomic Beam EIT

To improve the resolution of EIT resonances experiments were performed using the standard technique of a collimated atomic beam. Isotopically enriched ${}^6\text{Li}$ atoms are evaporated from an oven at a temperature of 450°C to produce a thermal atomic beam. At this temperature the ${}^6\text{Li}$ vapour pressure in the oven is expected to be 4×10^{-4} Torr. The diameter of the beam at the centre of the probe region is 7 mm. Ultra high vacuum of 2×10^{-10} Torr is achieved in an anti-reflection coated glass cell (for 670 nm) which has outer dimensions of $3 \times 3 \times 12\text{ cm}^3$ with a wall thickness of 3 mm. The collimated atomic beam is excited at right angles by resonant laser light in the interaction region. The pump and probe intensities were 1.4 mW/cm^2 for both beams. Fluorescence from atoms in the probe region was detected using a photomultiplier tube. The cell was wrapped in μ -metal to reduce stray magnetic fields.

4.1. Results

Resonant fluorescence in the collimated atomic beam showed a much narrower transverse Doppler width of 20 MHz compared to $\approx 3.5\text{ GHz}$ obtained in the vapour cell. Therefore, the hyperfine splitting of the $2^2\text{P}_{1/2}$ state of 26.1 MHz can be resolved. Figure 5 shows a plot of fluorescence of the D1 line as a function of frequency difference between the pump and probe laser. In this figure the probe laser is scanned over both the $F = 3/2 \rightarrow F' = 1/2$ and $F = 3/2 \rightarrow F' = 3/2$ transitions whereas the pump laser has a fixed frequency tuned to the $F = 1/2 \rightarrow F' = 1/2$ (a) or $F = 1/2 \rightarrow F' = 3/2$ (b) transition. The EIT dip is more pronounced when the fixed laser is tuned to the $F' = 3/2$ state which is due to the larger transition probability. For this reason we performed all of the subsequent experiments with the pump laser tuned to the $F = 1/2 \rightarrow F' = 3/2$ transition.

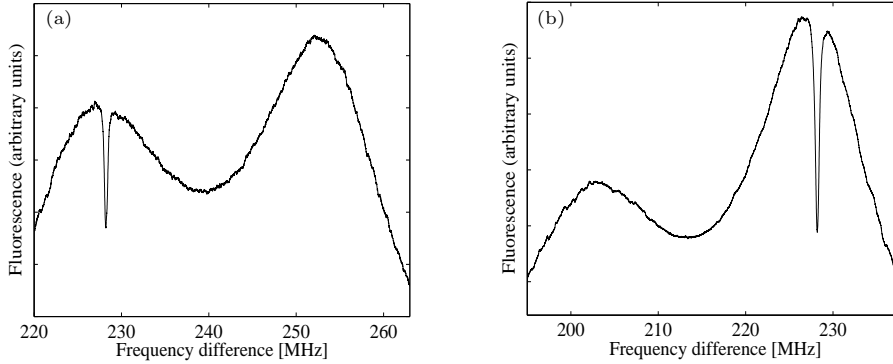


Figure 5. D1 line fluorescence from ${}^6\text{Li}$ atoms. Probe laser is scanned over both the $F = 3/2 \rightarrow F' = 1/2$ and $F = 3/2 \rightarrow F' = 3/2$ transitions. (a) Fixed pump laser tuned to (a) $F = 1/2 \rightarrow F' = 1/2$ transition and (b) $F = 1/2 \rightarrow F' = 3/2$ transition.

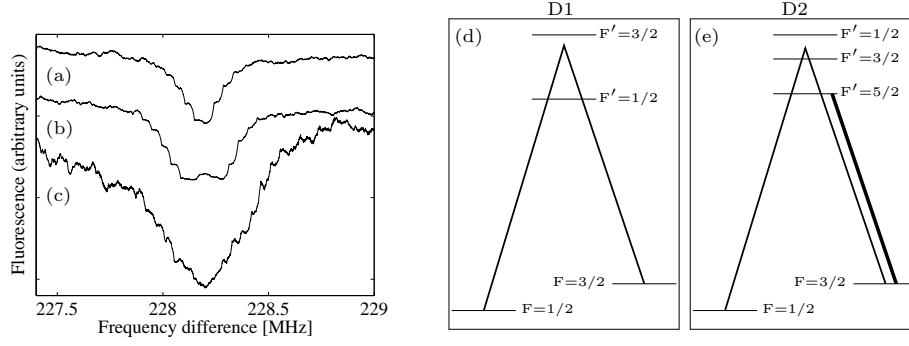


Figure 6. Fluorescence of the D1 and D2 line as a function of frequency difference between the pump and probe laser. (a) D1 resonance (width of 210 kHz) with applied magnetic field, (b) D1 resonance (370 kHz) with no magnetic field, (c) D2 resonance (560 kHz) with no magnetic field. The Raman transition responsible for the D1 and D2 resonance is shown in (d) and (e) respectively.

The EIT resonances obtained on the D1 and D2 lines are shown in figure 6. The intensity of the resonant fluorescence on the D2 line is higher, but the contrast of the sub-natural resonances with respect to the residual Doppler background is lower compared to the D1 line. In this regard the observations in the atomic beam and the vapour cell are very similar. However, better spectral resolution in the atomic beam allows us to demonstrate that the width of EIT resonances in both cases is also essentially different. The sub-natural resonances observed in the atomic beam on both lines under very similar experimental conditions such as light intensity, polarization and beam overlapping are shown in figure 6. The curve in figure 6 (c) represents EIT resonance observed on the D2 line without applied magnetic field. The width of the resonance is approximately 560 kHz. The sub-natural resonance on the D1 line (370 kHz) (figure 6 (b)) reveals a doublet structure due to residual magnetic field in the interaction region. This splitting is hidden on the D2 line by the large width of the EIT resonance. The double structure can be removed by applying a small magnetic field along the atomic beam resulting in the 210 kHz wide resonance (figure 6 (a)) on the D1 line. We believe that the EIT resonance on the D2 line is wider because of shorter lifetime of the ground state coherence destructed via the cycling transition $F = 3/2 \rightarrow F' = 5/2$.

Figure 7 shows several EIT resonances obtained for different polarizations with and without an applied magnetic field (≈ 2 G) along the atomic beam. In figure 7 (a) and figure 7 (b) the polarization of both lasers is linear and perpendicular to each other. The two outer peaks in figure 7 (b) are both shifted by 2Δ from the zero field resonance which is consistent with the Raman transitions depicted in figure 7 (c). In figure 7 (d) and figure 7 (e) the polarization of both laser beams are aligned parallel to each other and orthogonal to the magnetic field. Only two Λ -type Raman transitions are possible in this configuration (figure 7 (f)). The two resulting EIT resonances are both shifted by Δ to either side of the zero-magnetic field resonance. The amplitudes are much smaller when parallel polarization light was applied. This can be understood by considering that the atoms will undergo transitions between all Zeeman sublevels, but for parallel polarized pump and probe light, not all of these contribute to coherences

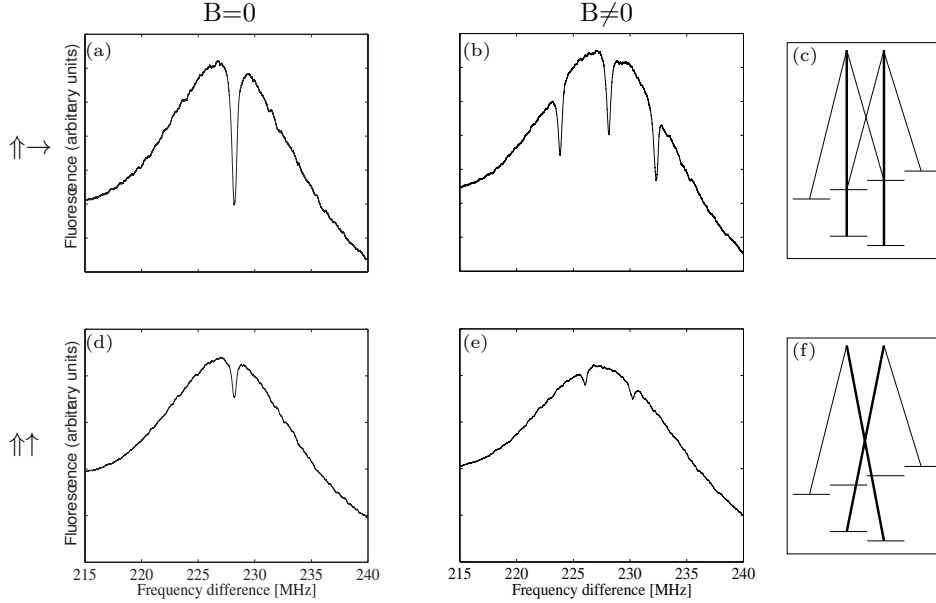


Figure 7. Fluorescence of the D1 line as a function of frequency difference. Fixed pump laser tuned to $F = 1/2 \rightarrow F' = 3/2$. (a) and (d): $B=0$, (b) and (e): $B \approx 2$ G. (a) and (b): linear perpendicular polarization, (d) and (e): linear parallel polarization. The transitions shown in (c) and (f) are responsible for each of the corresponding resonances to their left. The thicker lines represent the pump transitions.

(see figure 7 (f)). Similar results were obtained for the D2 line.

The EIT resonances in the ^6Li beam (figures 5 and 7) have a width of ≈ 300 kHz for the D1 line. This is a factor of 10 reduction compared to the vapour cell experiments. To get a better understanding of the broadening of our EIT resonances in the atomic beam we investigated the dependence of the width on the laser intensity of the pump laser, as shown in figure 8 (a). In addition, the amplitudes of the EIT resonances are shown. Note that the intensity of the probe laser is kept fixed at 1 mW/cm^2 . We observe a linear dependence of both the amplitude and the resonance width on the laser intensity. The linear behaviour of the resonance width is expected when power broadening becomes significant (Agap'ev 1993). Extrapolation gives a low-intensity limit of 190 kHz.

Additional broadening comes from the limited interaction time of the atoms with the light field (transit-time broadening). This was studied by measuring the resonance width for different laser beam cross-sections and the results are shown in figure 8(b). In our work the sum of the laser intensities was kept fixed at 1.7 mW/cm^2 . A significant increase could be observed for interaction lengths smaller than 5 mm. However, for the beam diameter of 18 mm used in all other experiments the broadening due to the transit time is negligible relative to the contribution of power broadening and magnetic field inhomogeneities.

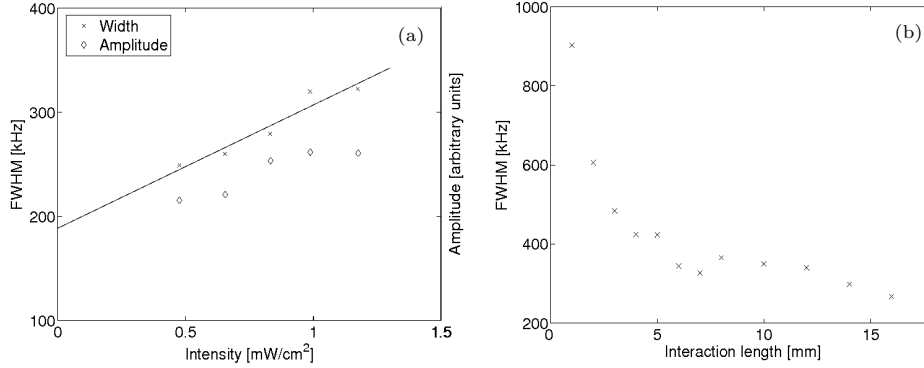


Figure 8. (a) Width of observed EIT resonance versus pump laser intensity. The intensity of the probe laser was fixed at 1 mW/cm^2 . The amplitude of the resonances as a function of laser intensity is also shown. (b) Width of observed EIT resonance versus interaction length. The sum of the laser intensities was 1.7 mW/cm^2 . In (a) and (b) EIT was achieved using the $^2P_{1/2}$, $F' = 3/2$ excited state and the polarization of the laser beams was linear and perpendicular to each other.

5. Ramsey Spectroscopy

Further reduction of EIT resonance widths was achieved using Ramsey spectroscopy (Ramsey 1989). In this technique atoms or molecules in a beam pass two spatially separated interaction regions. Optical Ramsey fringes were observed on beams of Na and Cs atoms pumped into coherent non-absorbing states (Thomas *et al* 1982, Hemmer *et al* 1993).

Here, a coherent superposition of the $F = 1/2$ and $F = 3/2$ ground states is prepared in a light field. The laser field consists of two co-propagating laser beams which are resonant with the $F = 1/2 \rightarrow F' = 3/2$ and $F = 3/2 \rightarrow F' = 3/2$ transitions. After some time the state is probed in a second interaction region consisting of the same two frequencies. Similar to the EIT experiments described previously, the laser resonant with the $F = 1/2 \rightarrow F' = 3/2$ transition is kept fixed while the other frequency is swept over the $F = 3/2 \rightarrow F' = 3/2$ transition.

In our experiment the two interaction regions were separated by $L = 7.7 \text{ mm}$. This was achieved by using only one laser beam in which the complete central vertical portion was blocked. Figure 9 shows a plot of fluorescence as a function of frequency difference. The intensities for both pump and probe were 2 mW/cm^2 . The polarization of both beams were linear and perpendicular to each other. To amplify the Ramsey fringes the laser light in the first interaction region was chopped, while the fluorescence of the probe region was detected by a photo multiplier tube using a lock-in amplifier. The obtained width (FWHM) of the resonance was narrower than 100 kHz which is consistent with calculations based on a mean atomic velocity $v \approx 1600 \text{ ms}^{-1}$ and a laser field separation L : $\Delta\nu = v/(3L) = 70 \text{ kHz}$ (Demtröder 2003).

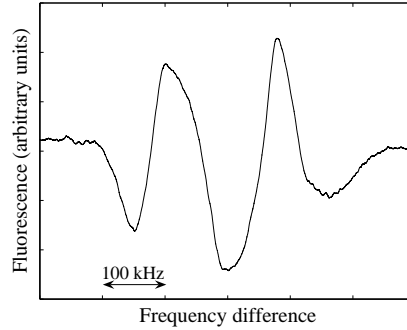


Figure 9. Optical Ramsey fringes of two co-propagating laser beams in a Raman-type configuration.

6. Summary

We have reported electromagnetically induced transparency in ${}^6\text{Li}$ in both the vapour cell and atomic beam. Resonant light with two frequency components was used to produce coherences between the two hyperfine levels in the ${}^6\text{Li}$ ground state for the first time, allowing fluorescence resonances as narrow as 200 kHz to be observed. The effects of various optical polarization configurations and applied magnetic fields were investigated, and these were readily interpreted with Λ -type Raman transitions. It has been found that the maximum contrast of the sub-natural resonances of suppressed fluorescence occurs for orthogonal linear Zeeman polarizations of the probe and pump components. Magnetic field insensitive fluorescence resonance (in the linear approximation) has been demonstrated despite the fact that the $m = 0 \rightarrow m' = 0$ -type Raman transition does not exist for ${}^6\text{Li}$.

The EIT resonances for the D2 line have been observed in spite of destructive excitation via cycling transition. However, the sub-natural resonances are weaker and broader compared to the D1 line. Additional experiments using the Ramsey separated field technique showed further reduction in the width of the EIT resonances. As an alkali atom with integer nuclear spin, fermionic ${}^6\text{Li}$ presents a potentially interesting system in which to investigate coherence effects such as EIT. Its energy level scheme differs from other atomic species previously investigated, in terms of the number of hyperfine excited states and their small energy splitting. The results reported here are consistent with coherence effects observed using other alkali atoms, such as Rb and Cs, although the smaller hyperfine splitting of ${}^6\text{Li}$ has allowed significant experimental simplification. Our initial atomic coherence investigations on this previously unexplored isotope provide a basis for additional studies.

Acknowledgments

We would like to thank Peter Hannaford for his useful advice and discussions. This project is supported by the Australian Research Council Centre of Excellence for Quantum-Atom Optics and Swinburne University of Technology.

References

- Agap'ev B D, Gornyi M B, Matisov B G, Rozhdestvenskii Yu V 1993 *Usp. Fiz. Nauk* **163** 1–36
- Akulshin A M, Cinnino A, Sidorov A I, McLean R and Hannaford P 2003 *Journal of Optics B-Quantum and Semiclassical Optics* **5** S479–S485
- Arimondo E 1996 *Prog. Opt.* **30** 257–354
- Demtröder W 2003 *Laser spectroscopy: Basic concepts and Instrumentation* vol 3 (New Delhi: Springer-Verlag)
- Harris S E 1997 *Physics Today* **50**(7) 32
- Harris S E and Hau L 1999 *Phys. Rev. Lett.* **82** 4611–4614
- Hemmer P R, Shahriar M S, Lamela-Rivera H, Smith S P, Bernacki B E and Ezekiel S 1993 *J. Opt. Soc. Am. B* **10** 1326
- Knappe S, Schwindt P D D, Shah V, Hollberg L, Kitching J, Liew L and Moreland J 2005 *Optics Express* **13** 1249–1253
- Lukin M D 2003 *Rev. Mod. Phys.* **75** 457–472
- Magnus F, Boatwright A L, Flodin A and Shiell R C 2005 *J. Opt. B:Quantum Semiclass. Opt.* **7** 109–118
- Matsko A B, Kocharovskaya O, Rostovtsev Y, Welch G R, Zibrov A S and Scully M O 2001 *Advances in Atomic Mol. and Opt. Phys.* **46** 191–242
- McAlexander W I, Abraham E R I, and Hulet R G 1996 *Phys. Rev. A* **54** R5–R8
- Ramsey N F 1989 *Molecular Beams* 2nd Edn, Clarendon, Oxford
- Schmidt O, Wynands R, Hussein Z and Meschede D 1996 *Phys. Rev. A* **53** R27–R30
- Stähler M, Wynands R, Knappe S, Kitching J, Hollberg L, Taichenachev A and Yudin V *Opt. Lett.* **27** 1472–1474
- Thomas J E, Hemmer P R, Ezekiel S, Leiby C C Jr., Picard R H and Willis C R 1982 *Phys. Rev. Lett.* **48** 867–870
- Walls J, Ashby R, Clarke J J, Lu B and van Wijngaarden W A 2003 *European Physics Journal D* **22** 159–162
- Wynands R and Nagel A 1999 *Appl. Phys. B* **68** 1–25
- van Wijngaarden W A 2005 *Can. J. Phys.* **83** 327
- Zibrov A S, Lukin M D, Nibonov D E, Hollberg L, Scully M O, Velichansky V L and Robinson H G 1995 *Phys. Rev. Lett.* **75** 1499–1502